Langmuir

Article

pubs.acs.org/Langmuir

Evaporation of Droplets on Strongly Hydrophobic Substrates

Jutta M. Stauber, Stephen K. Wilson,* and Brian R. Duffy

Department of Mathematics and Statistics, University of Strathclyde, Livingstone Tower, 26 Richmond Street, Glasgow, G1 1XH, United Kingdom

Khellil Sefiane

School of Engineering, University of Edinburgh, The King's Buildings, Mayfield Road, Edinburgh, EH9 3JL, United Kingdom

International Institute for Carbon-Neutral Energy Research (WPI-I2CNER), Kyushu University, 744 Motooka, Nishi-ku, Fukuoka 819-0395, Japan

ABSTRACT: The manner in which the extreme modes of droplet evaporation (namely, the constant contact radius and the constant contact angle modes) become indistinguishable on strongly hydrophobic substrates is described. Simple asymptotic expressions are obtained which provide good approximations to the evolutions of the contact radius, the contact angle, and the volume of droplets evaporating in the extreme modes for a wide range of hydrophobic substrates. As a consequence, on strongly hydrophobic substrates it is appropriate to use the so-called "2/3 power law" to extrapolate the lifetimes of droplets evaporating in the constant contact radius mode as well as in the constant contact angle mode.

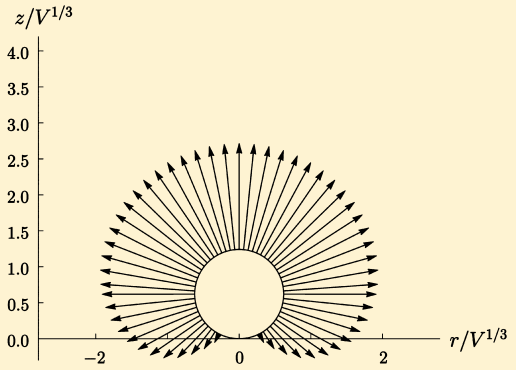

1. INTRODUCTION

As, for example, the recent review articles by Cazabat and Guéna,[1] Erbil,[2] and Larson[3] demonstrate, the evaporation of a fluid droplet on a solid substrate has been the subject of extensive ongoing theoretical and experimental investigations by a wide range of research groups in recent years.

As many authors have shown, after a short transient in which a droplet deposited onto a substrate rapidly adjusts to a quasi-equilibrium shape with initial contact radius R_0 and initial contact angle θ_0, the droplet can evaporate in a wide variety of modes. The most extreme modes of evaporation are the so-called "constant contact radius" (CR) mode, in which the contact line is always pinned and the contact angle $\theta = \theta(t)$ decreases while the contact radius $R(t) = R_0$ remains constant, and the so-called "constant contact angle" (CA) mode, in which the contact line is always depinned and the contact radius $R = R(t)$ decreases while the contact angle $\theta(t) = \theta_0$ remains constant, where t denotes time. As the pioneering studies of Picknett and Bexon[4] and Bourgès-Monnier and Shanahan[5] and many subsequent works have shown, in practice, droplets often evaporate in a "stick-slide" (SS) mode, which involves some combination of "stick" (i.e., with a pinned contact line) and "slide" (i.e., with a depinned contact line) phases. Recently Nguyen and Nguyen,[6,7] Dash and Garimella,[8] and Stauber et al.[9,10] have formulated and analyzed a simple yet effective model for an idealized SS mode consisting of a single stick phase followed by a single slide phase. Nevertheless, understanding the extreme modes remains a key part of understanding the evaporation of droplets.

The main aim of the present work is to show how the extreme modes of droplet evaporation converge as the value of the initial contact angle θ_0 increases toward π, and so, in particular, to describe the manner in which they become indistinguishable on strongly hydrophobic substrates.

2. THE MATHEMATICAL MODEL

The widely used "diffusion-limited" model employed in the present work is based on the assumption that the evaporation from the droplet is quasi-steady and limited by the diffusion of vapor in the quiescent atmosphere above it. This model, together with the assumption that the droplet is sufficiently small that gravitational effects are negligible and hence its free surface is a spherical cap, has been the basis for work by a large number of previous authors, notably Picknett and Bexon,[4] Coutant and Penski,[11] Deegan et al.,[12,13] Erbil et al.,[14] Hu and Larson,[15] Popov,[16] Dunn et al.,[17,18] Masoud and Felske,[19] Sefiane et al.,[20] Shin et al.,[21] Eggers and Pismen,[22] Semenov et al.,[23−25] Doganci et al.,[26] Gelderblom et al.,[27,28] Sobac and Brutin,[29,30] Song et al.,[31] Nguyen et al.,[32] Nguyen and Nguyen,[6,7,33,34] Talbot et al.,[35] Yu et al.,[36] Dash and Garimella,[8,37] Stauber et al.,[9,10] Trybala et al., and Gatapova et al.[40]

Referred to cylindrical polar coordinates (r,z) with origin on the substrate at the center of the droplet, its free surface, denoted

Received: January 23, 2015
Revised: March 6, 2015
Published: March 9, 2015

DOI: 10.1021/acs.langmuir.5b00286
Langmuir 2015, 31, 3653−3660

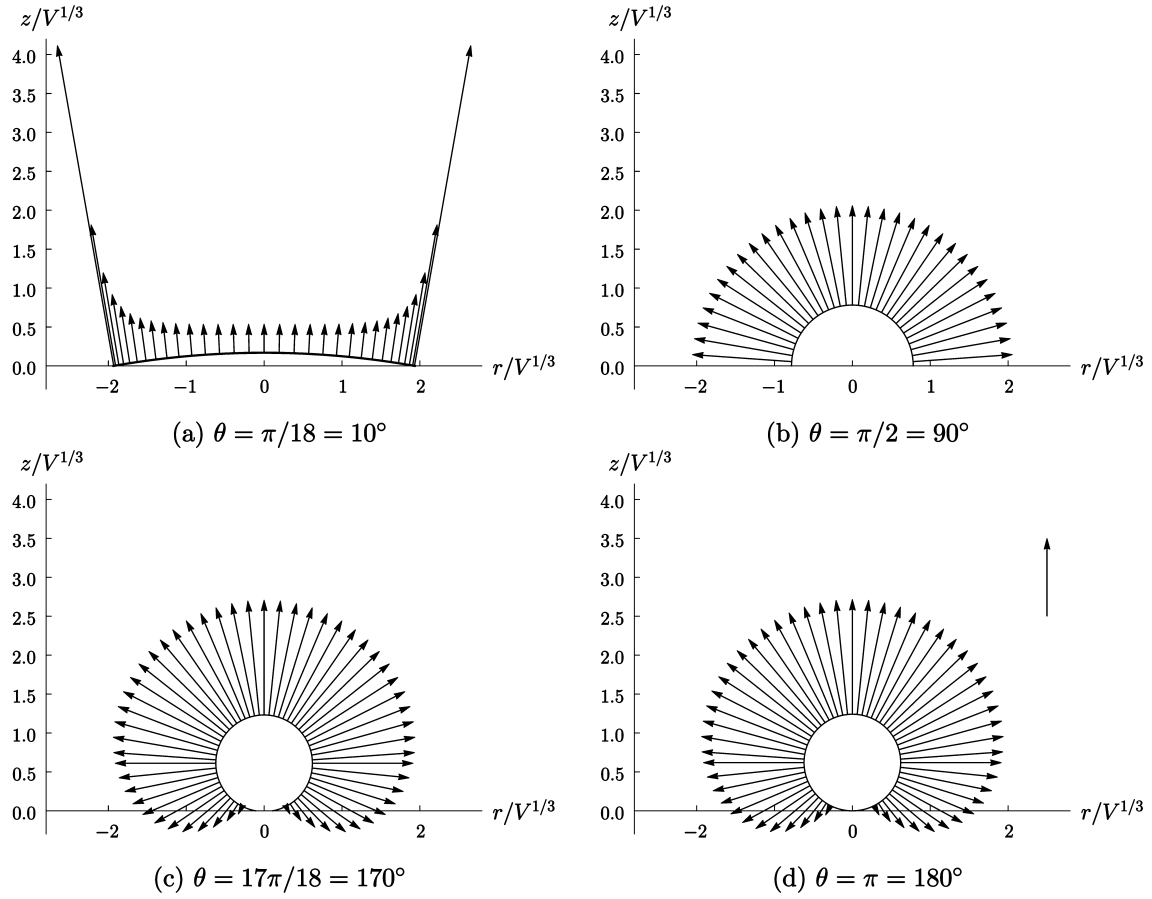

Figure 1. Scaled plots of four droplets given by eq 1, each with the same volume, V, but different contact angles, namely, (a) $\theta = \pi/18 = 10°$, (b) $\theta = \pi/2 = 90°$, (c) $\theta = 17\pi/18 = 170°$, and (d) $\theta = \pi = 180°$, and different scaled contact radii, $R/V^{1/3}$, together with the corresponding scaled evaporative flux from the free surface, $JV^{1/3}/(D(c_{sat}-c_\infty))$, given by eq 3 or, in the special case $\theta = \pi$, by eq 7, shown by the arrows. Note that the length of the arrows is proportional to the magnitude of $JV^{1/3}/(D(c_{sat}-c_\infty))$, with the length of the reference arrow in panel d corresponding to $JV^{1/3}/(D(c_{sat} - c_\infty)) = 1$.

by $z = h(r,t)$, is a spherical cap with radius $\mathcal{R} = \mathcal{R}(t)$ ($\mathcal{R} \geq R$), contact radius $R = R(t)$ ($R \geq 0$), and contact angle $\theta = \theta(t)$ ($0 \leq \theta \leq \pi$) given by

$$h = -\mathcal{R}\cos\theta \pm \sqrt{\mathcal{R}^2 - r^2} \quad \text{where} \quad \mathcal{R} = \frac{R}{\sin\theta} \tag{1}$$

Note that the physically relevant (i.e., the non-negative) part of h given by eq 1 is a single-valued function of r for $0 \leq r \leq R$ when $0 \leq \theta \leq \pi/2$ and for $0 \leq r < R$ when $\pi/2 < \theta \leq \pi$ (in which case only the "+" sign is relevant), but a double-valued function of r for $R \leq r < \mathcal{R}$ when $\pi/2 < \theta \leq \pi$ (in which case the "+" and "−" signs correspond to the upper and lower hemispheres, respectively). The volume of the droplet, $V = V(t)$, is given by

$$V = 2\pi\int_0^R h\, r\, \mathrm{d}r = \frac{\pi R^3}{3}\frac{\sin\theta(2 + \cos\theta)}{(1 + \cos\theta)^2} \tag{2}$$

Since the evaporation is assumed to be quasi-steady and limited by the diffusion of vapor in the atmosphere, the vapor concentration in the atmosphere, $c = c(r,z,t)$, satisfies Laplace's equation, $\nabla^2 c = 0$, subject to the boundary conditions that at the free surface of the droplet the atmosphere is saturated with vapor and so c takes its saturation value, c_{sat}, that far away from the droplet c takes its constant ambient value, c_∞ ($0 \leq c_\infty \leq c_{sat}$), and that the vapor cannot penetrate the substrate (i.e., $\partial c/\partial z = 0$ on $z = 0$ for $r > R$). In the simplest and most widely used version of the model employed here, c_{sat} is assumed to be constant; we will discuss the validity of this assumption in Section 5. As several previous authors (see, for example, Popov[16]) describe, the solution for c is given by Lebedev's[41] solution for a mathematically equivalent electrostatics problem. In particular, the evaporative flux from the free surface of the droplet, $J = J(r,t)$, defined by $J = -D\mathbf{n}\cdot\nabla c$, where $\mathbf{n}$ is the unit outward normal to the free surface and D is the diffusion coefficient of vapor in the atmosphere, is given by

$$J = \frac{D(c_{sat} - c_\infty)}{R}\left[\frac{1}{2}\sin\theta + \sqrt{2}\,(\cosh\alpha + \cos\theta)^{3/2} \times \int_0^\infty \frac{\tau\cosh\theta\tau}{\cosh\pi\tau}\tanh[\tau(\pi - \theta)]P_{-1/2+i\tau}(\cosh\alpha)\,\mathrm{d}\tau\right] \tag{3}$$

where $P_{-1/2+i\tau}(\cosh\alpha)$ denotes the Legendre function of the first kind of degree $-1/2 + i\tau$ and argument

$$\cosh\alpha = \frac{r^2\cos\theta \pm R\sqrt{R^2 - r^2\sin^2\theta}}{R^2 - r^2} \tag{4}$$

where again the "+" and "−" signs correspond to the upper and lower hemispheres, respectively, when $\pi/2 < \theta \leq \pi$.

At leading order in the limit of small contact angle, $\theta \to 0^+$, the free surface of the droplet is a parabola, namely, $h = \theta(R^2 - r^2)/(2R)$, and the flux is given by

DOI: 10.1021/acs.langmuir.5b00286
Langmuir 2015, 31, 3653−3660

$$J = \frac{2}{\pi}\frac{D(c_{sat} - c_\infty)}{\sqrt{R^2 - r^2}} \tag{5}$$

(see, for example, Popov[16]). In the special case $\theta = \pi/2$ the free surface of the droplet is a hemisphere with radius $\mathcal{R} = R$, namely, $h = (R^2 - r^2)^{1/2}$, and the flux is uniform and given by

$$J = \frac{D(c_{sat} - c_\infty)}{R} \tag{6}$$

(see, for example, Popov[16]).

In the special case $\theta = \pi$ the free surface of the droplet is a complete sphere of radius $\mathcal{R}$ ($\mathcal{R} \geq 0$) with zero contact radius, $R = 0$, namely, $h = \mathcal{R} \pm (\mathcal{R}^2 - r^2)^{1/2}$. In this case the expression for the flux (eq 3) requires careful interpretation, and so it is more convenient to use Smith and Barakat's[42] solution for a mathematically equivalent electrostatics problem to obtain (after some simplification)

$$J = \frac{D(c_{sat} - c_\infty)}{2\mathcal{R}}\left[1 + \left(\frac{2\mathcal{R}}{h}\right)^{3/2}\int_0^\infty q \tanh q\, J_0\left(\frac{rq}{h}\right)\exp(-q)\, dq\right] \tag{7}$$

where $J_0(\cdot)$ denotes the Bessel function of the first kind of order zero. In particular, the flux from the apex of the droplet, $r = 0$, is given by

$$J = \frac{D(c_{sat} - c_\infty)}{\mathcal{R}}\text{Catalan} \tag{8}$$

where Catalan $\simeq 0.9160$ is Catalan's constant.

Following Deegan et al.,[12] Gelderblom et al.[28] showed that near the contact line, $r = R$ and $z = 0$, the flux is given by

$$J \sim A(\theta)\frac{D(c_{sat} - c_\infty)}{R}\left(\frac{R - r}{R\cos\theta}\right)^\lambda \quad \text{where}$$
$$\lambda = \frac{2\theta - \pi}{2\pi - 2\theta} \quad \text{as} \quad r \to R \tag{9}$$

where the function $A = A(\theta)$ can, in principle, be calculated from eq 3. In particular, eq 9 shows that the behavior of the flux near the contact line depends qualitatively (rather than just quantitatively) on the value of the contact angle. Specifically, when $0 \leq \theta < \pi/2$, then $-1/2 \leq \lambda < 0$, and so the flux is (integrably) singular at the contact line; when $\theta = \pi/2$, then $\lambda = 0$, and so the flux is finite at the contact line; and when $\pi/2 < \theta \leq \pi$, then $\lambda > 0$, and so the flux is zero at the contact line.

Figure 1 shows scaled plots of four droplets given by eq 1 each with the same volume, V, but different contact angles, namely, $\theta = \pi/18 = 10°$ (typical of $0 \leq \theta < \pi/2$), $\theta = \pi/2 = 90°$, $\theta = 17\pi/18 = 170°$ (typical of $\pi/2 < \theta < \pi$), and $\theta = \pi = 180°$, and different scaled contact radii, $R/V^{1/3}$, together with the corresponding scaled evaporative flux from the free surface, $J V^{1/3}/(D(c_{sat} - c_\infty))$, given by eq 3 or, in the special case $\theta = \pi$, by eq 7, shown by the arrows. In particular, Figure 1 clearly illustrates the qualitatively different behavior of the flux near the contact line in the cases $0 \leq \theta < \pi/2$, $\theta = \pi/2$, and $\pi/2 < \theta \leq \pi$ described above. Specifically, Figure 1 shows that the diffusion-limited model predicts that, when $0 \leq \theta < \pi/2$, the flux is largest (theoretically infinite) at the contact line and smallest at the apex of the droplet (i.e., at $r = 0$), when $\theta = \pi/2$ the flux is uniform and given by eq 6, and when $\pi/2 < \theta \leq \pi$, the flux is largest at the apex of the droplet and smallest (theoretically zero) at the contact line.

3. THE EVOLUTION OF THE DROPLET

Integrating the flux J given by eq 3 over the free surface of the droplet gives the total flux from the droplet at any instant, and so the rate of change of the volume of the droplet, dV/dt, is given by

$$\frac{dV}{dt} = -\frac{\pi R D(c_{sat} - c_\infty)}{\rho}\frac{g(\theta)}{(1 + \cos\theta)^2} \tag{10}$$

where V is given in terms of R and θ by eq 2, and the function $g = g(\theta)$ is defined by

$$g(\theta) = (1 + \cos\theta)^2\left\{\tan\frac{\theta}{2} + 8\int_0^\infty \frac{\cosh^2\theta\tau}{\sinh 2\pi\tau}\tanh[\tau(\pi - \theta)]\, d\tau\right\} \tag{11}$$

In particular, the function g satisfies $g(0) = 16/\pi$, $g(\pi/2) = 2$, and $g \sim (\pi - \theta)^3 \ln 2 \to 0^+$ as $\theta \to \pi^-$.

Equation 10 determines the evolution of V, and hence the evolution of R and/or θ as the droplet evaporates, and hence, in particular, the lifetime of the droplet (i.e., the time it takes for R and/or θ and hence for V to reach zero).

As several previous authors have described, for a droplet evaporating in the CR mode, $R = R_0$ is constant, and so eq 10 becomes an equation for $\theta = \theta(t)$, namely,

$$\frac{d\theta}{dt} = -\frac{D(c_{sat} - c_\infty)}{\rho R_0^2}g(\theta) \tag{12}$$

which has the implicit solution

$$t = \frac{\rho R_0^2}{D(c_{sat} - c_\infty)}\int_\theta^{\theta_0}\frac{d\theta}{g(\theta)} \tag{13}$$

while for a droplet evaporating in the CA mode, $\theta = \theta_0$ is constant, and so eq 10 becomes an equation for $R = R(t)$, namely,

$$\frac{dR}{dt} = -\frac{D(c_{sat} - c_\infty)}{\rho R}\frac{g(\theta_0)}{\sin\theta_0(2 + \cos\theta_0)} \tag{14}$$

which has the exact solution

$$R^2 = R_0^2 - \frac{2D(c_{sat} - c_\infty)}{\rho}\frac{g(\theta_0)}{\sin\theta_0(2 + \cos\theta_0)}t \tag{15}$$

and hence

$$V = \frac{\pi}{3}\frac{\sin\theta_0(2 + \cos\theta_0)}{(1 + \cos\theta_0)^2} \times\left[R_0^2 - \frac{2D(c_{sat} - c_\infty)}{\rho}\frac{g(\theta_0)}{\sin\theta_0(2 + \cos\theta_0)}t\right]^{3/2} \tag{16}$$

A key observation is that in the special case $\theta_0 = \pi$ (i.e., for a perfectly hydrophobic substrate) *the CR and CA modes coincide at all times t*. In this case, the free surface of the droplet is a complete sphere of radius $\mathcal{R} = \mathcal{R}(t)$ ($\mathcal{R} \geq 0$) touching the substrate at the single point $r = 0$ with constant contact radius $R \equiv R_0 = 0$ *and* constant contact angle $\theta \equiv \theta_0 = \pi$ *throughout its entire lifetime*, i.e., in this case (and only in this case) *the CR and CA modes are identical throughout their entire lifetimes*. Integrating the expression for the flux J in this special case given by eq 7 over the free surface of the droplet yields an equation for $\mathcal{R} = \mathcal{R}(t)$, namely,

$$\frac{d\mathcal{R}}{dt} = -\frac{D(c_{sat} - c_\infty)\ln 2}{\rho\mathcal{R}} \tag{17}$$

DOI: 10.1021/acs.langmuir.5b00286
Langmuir 2015, 31, 3653−3660

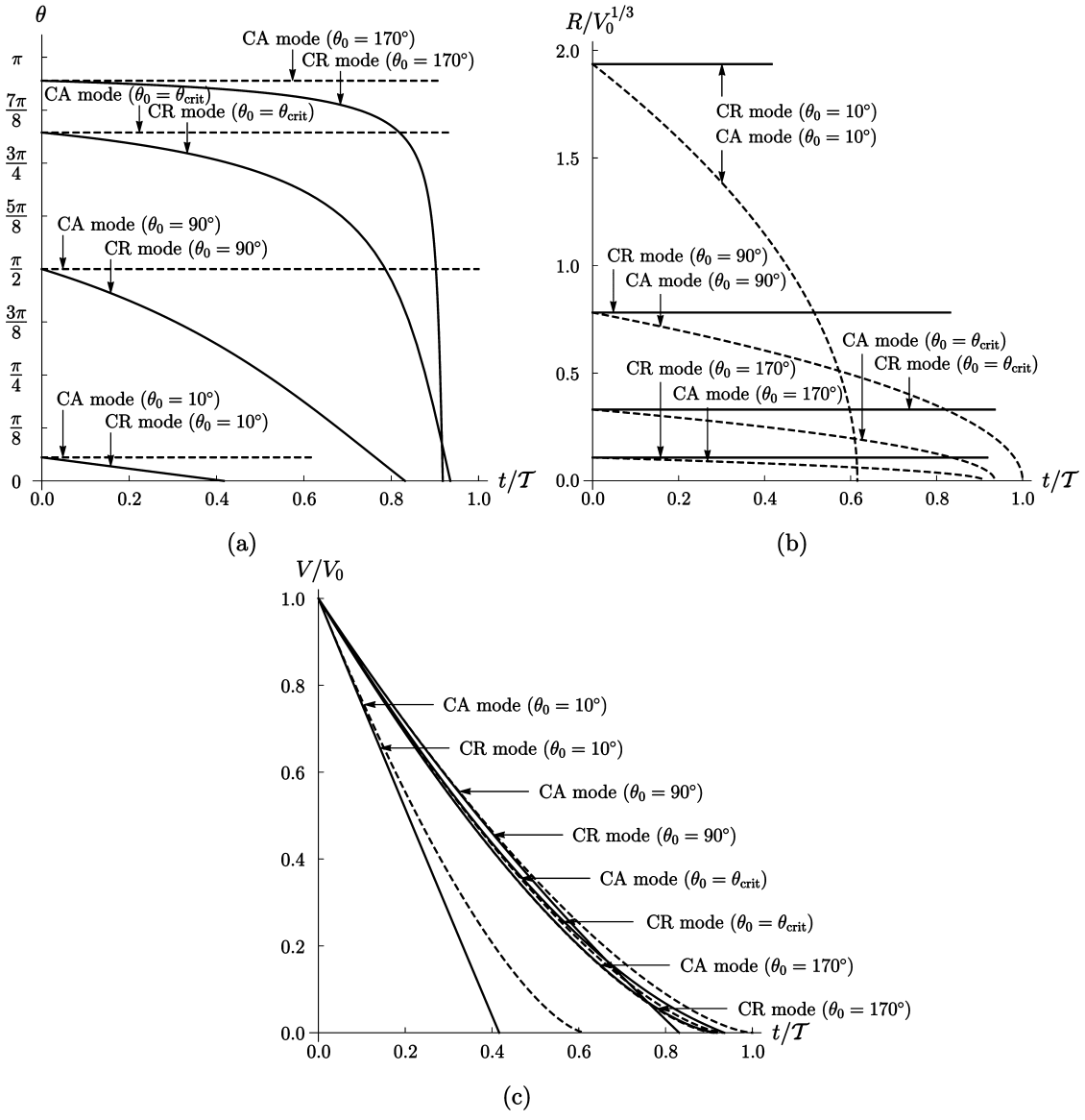

Figure 2. Evolutions of (a) the contact angle θ, (b) the scaled contact radius $R/V_0^{1/3}$, and (c) the scaled volume V/V_0, plotted as functions of scaled time $t/\mathcal{T}$ for droplets with different initial contact angles, namely, $\theta_0 = \pi/18 = 10°$, $\theta_0 = \pi/2 = 90°$, $\theta_0 = \theta_{crit} \simeq 2.5830 \simeq 148°$, and $\theta_0 = 17\pi/18 = 170°$, evaporating in the CR and CA modes, shown by solid and dashed lines, respectively.

which has the exact solution

$$\mathcal{R}^2 = \mathcal{R}_0^2 - \frac{2D(c_{sat} - c_\infty)\ln 2}{\rho}t \tag{18}$$

where $\mathcal{R}_0 = \mathcal{R}(0)$ is the initial radius of the sphere, and hence

$$V = \frac{4\pi\mathcal{R}^3}{3} = \frac{4\pi}{3}\left[\mathcal{R}_0^2 - \frac{2D(c_{sat} - c_\infty)\ln 2}{\rho}t\right]^{3/2} \tag{19}$$

To simplify the subsequent presentation it is convenient to scale time t with the maximum lifetime of a droplet evaporating in the CA mode (which occurs for $\theta_0 = \pi/2$), namely,

$$\mathcal{T} = \frac{\rho}{2D(c_{sat} - c_\infty)}\left(\frac{3V_0}{2\pi}\right)^{2/3} = \frac{\rho R_0^2}{2D(c_{sat} - c_\infty)}\left(\frac{\sin\theta_0(2 + \cos\theta_0)}{2(1 + \cos\theta_0)^2}\right)^{2/3} \tag{20}$$

where $V_0 = V(0)$ is the initial volume of the droplet.

Setting $\theta = 0$ in eq 13 yields an expression for the scaled lifetime of a droplet evaporating in the CR mode, namely,

$$t_{CR} = \left(\frac{2(1 + \cos\theta_0)^2}{\sin\theta_0(2 + \cos\theta_0)}\right)^{2/3}\int_0^{\theta_0}\frac{2\,d\theta}{g(\theta)} \tag{21}$$

and setting $R = 0$ in eq 15 or $V = 0$ in eq 16 yields an expression for the scaled lifetime of a droplet evaporating in the CA mode, namely,

$$t_{CA} = \left(\frac{2(1 + \cos\theta_0)^2}{\sin\theta_0(2 + \cos\theta_0)}\right)^{2/3}\frac{\sin\theta_0(2 + \cos\theta_0)}{g(\theta_0)} \tag{22}$$

Setting $\mathcal{R} = 0$ in eq 18 or $V = 0$ in eq 19 (or, equivalently, taking the limit $\theta_0 \to \pi^-$ in eq 21 or 22) yields an expression for the scaled lifetime of both modes when $\theta_0 = \pi$, namely, $t_{CA} = t_{CR} = t_\pi$, where

DOI: 10.1021/acs.langmuir.5b00286
Langmuir 2015, 31, 3653−3660

$$t_\pi = \frac{1}{4^{1/3}\ln 2} \simeq 0.9088 \tag{23}$$

(see Stauber et al.[10]).

Figure 2 shows the evolutions of θ, $R/{V_0}^{1/3}$, and V/V_0 plotted as functions of $t/\mathcal{T}$ for droplets with different initial contact angles, namely, $\theta_0 = \pi/18 = 10°$, $\theta_0 = \pi/2 = 90°$, $\theta_0 = \theta_{crit} \simeq 2.5830 \simeq 148°$, and $\theta_0 = 17\pi/18 = 170°$, evaporating in the CR and CA modes. In particular, Figure 2 shows that in the special case $\theta_0 = \theta_{crit}$ (first identified approximately by Picknett and Bexon[4] using an approximate expression for $g(\theta)$), the values of t_{CR} and t_{CA} coincide (specifically, $t_{CR} = t_{CA} = t_{crit} \simeq 0.9354$), but the evolutions of R, θ, and V for the two modes are very different. Note that this behavior is qualitatively different from that when $\theta_0 = \pi$ described previously for which the two modes are identical for their entire lifetimes.

Figure 3a shows the scaled lifetimes of droplets evaporating in the CR mode, t_{CR}, given by eq 21, and in the CA mode, t_{CA}, given by eq 22, plotted as functions of the initial contact angle θ_0. In particular, Figure 3a illustrates the sometimes overlooked fact that the lifetime of the CR mode is (slightly) longer than that of the CA mode when $\theta_{crit} < \theta_0 < \pi$ (see Picknett and Bexon[4]), and shows that both t_{CR} and t_{CA} approach t_π from above as $\theta_0 \to \pi^-$. In fact, analysis of the expressions for t_{CR} and t_{CA} given by eqs 21 and 22, respectively, in the limit $\theta_0 \to \pi^-$ reveals that

$$t_{CR} = t_\pi\left[1 - \frac{4\ln 2 - 1}{12\ln 2}(\pi - \theta_0)^2 \ln(\pi - \theta_0)\right] + O(\pi - \theta_0)^2 \tag{24}$$

and

$$t_{CA} = t_\pi\left[1 + \frac{4\ln 2 - 1}{24\ln 2}(\pi - \theta_0)^2\right] + O(\pi - \theta_0)^4 \tag{25}$$

(see Stauber et al.[10]). Figure 3b is an enlargement of Figure 3a near $\theta_0 = \pi$ also showing the asymptotic expressions 24 and 25, and illustrates that both asymptotic expressions, but particularly that for t_{CA}, provide good approximations to the exact values of t_{CR} and t_{CA} for a reasonably wide range of values of θ_0 near π.

4. THE CONVERGENCE OF THE EXTREME MODES

The evolutions of θ and $R/{V_0}^{1/3}$ plotted in Figure 2a,b show that as the value of the initial contact angle θ_0 increases toward π both the value of the (varying) contact angle θ in the CR mode and the value of the (varying) contact radius R in the CA mode stay increasingly close to their initial values θ_0 and R_0, respectively. In other words, the extreme modes of droplet evaporation converge as the value of θ_0 increases toward π, and so, in particular, *the extreme modes become indistinguishable on strongly hydrophobic substrates.*

This behavior might have been expected for the CA mode, for which $\theta \equiv \theta_0 \approx \pi$ necessarily remains close to π and R decreases by a small amount from its small initial value of $R_0 \approx 0$ to zero, and hence necessarily remains close to its value $R \equiv 0$ in the special case $\theta_0 = \pi$ during its evolution. Indeed, analysis of eq 14 or 15 reveals that for a droplet evaporating in the CA mode, the asymptotic expression for the contact radius R is given by

$$R = \left(\frac{3V_0}{4\pi}\right)^{1/3}\left(1 - \frac{t}{t_\pi}\right)^{1/2}(\pi - \theta_0) + O(\pi - \theta_0)^3 \tag{26}$$

in the limit $\theta_0 \to \pi^-$, which remains close to $R = 0$ for the entire lifetime of the droplet (i.e., until $t = t_\pi$ at leading order).

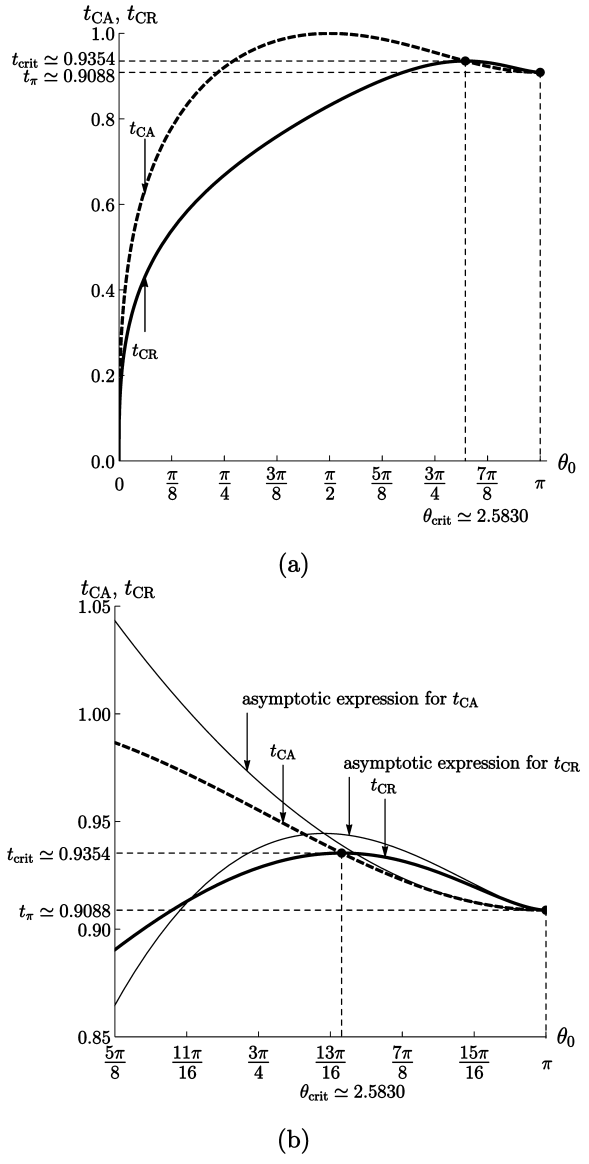

Figure 3. (a) Scaled lifetimes of droplets evaporating in the CR mode, t_{CR}, given by eq 21 and shown with a solid line, and in the CA mode, t_{CA}, given by eq 22 and shown with a dashed line, plotted as functions of the initial contact angle θ_0. (b) An enlargement of panel a near $\theta_0 = \pi$ also showing the asymptotic expressions for t_{CR} and t_{CA} in the limit $\theta_0 \to \pi^-$ given by eqs 24 and 25, respectively.

However, this behavior is not so immediately obvious for the CR mode, for which $R \equiv R_0 \approx 0$ necessarily remains small, but θ decreases by a nonsmall amount from its initial value of $\theta_0 \approx \pi$ to zero during its evolution. However, analysis of eq 12 reveals that for a droplet evaporating in the CR mode, the asymptotic expression for the contact angle θ is given by

$$\theta = \pi - \left(1 - \frac{t}{t_\pi}\right)^{-1/2}(\pi - \theta_0) + O(\pi - \theta_0)^3 \tag{27}$$

in the limit $\theta_0 \to \pi^-$, which indeed remains close to $\theta = \pi$ until near the end of its lifetime (i.e., until near to $t = t_\pi$ at leading order).

Furthermore, as the evolution of V in the case $\theta_0 = 17\pi/18 = 170°$ shown in Figure 2c shows, V decreases from V_0 to zero in a very similar manner for both extreme modes, and indeed for this

DOI: 10.1021/acs.langmuir.5b00286
Langmuir 2015, 31, 3653−3660

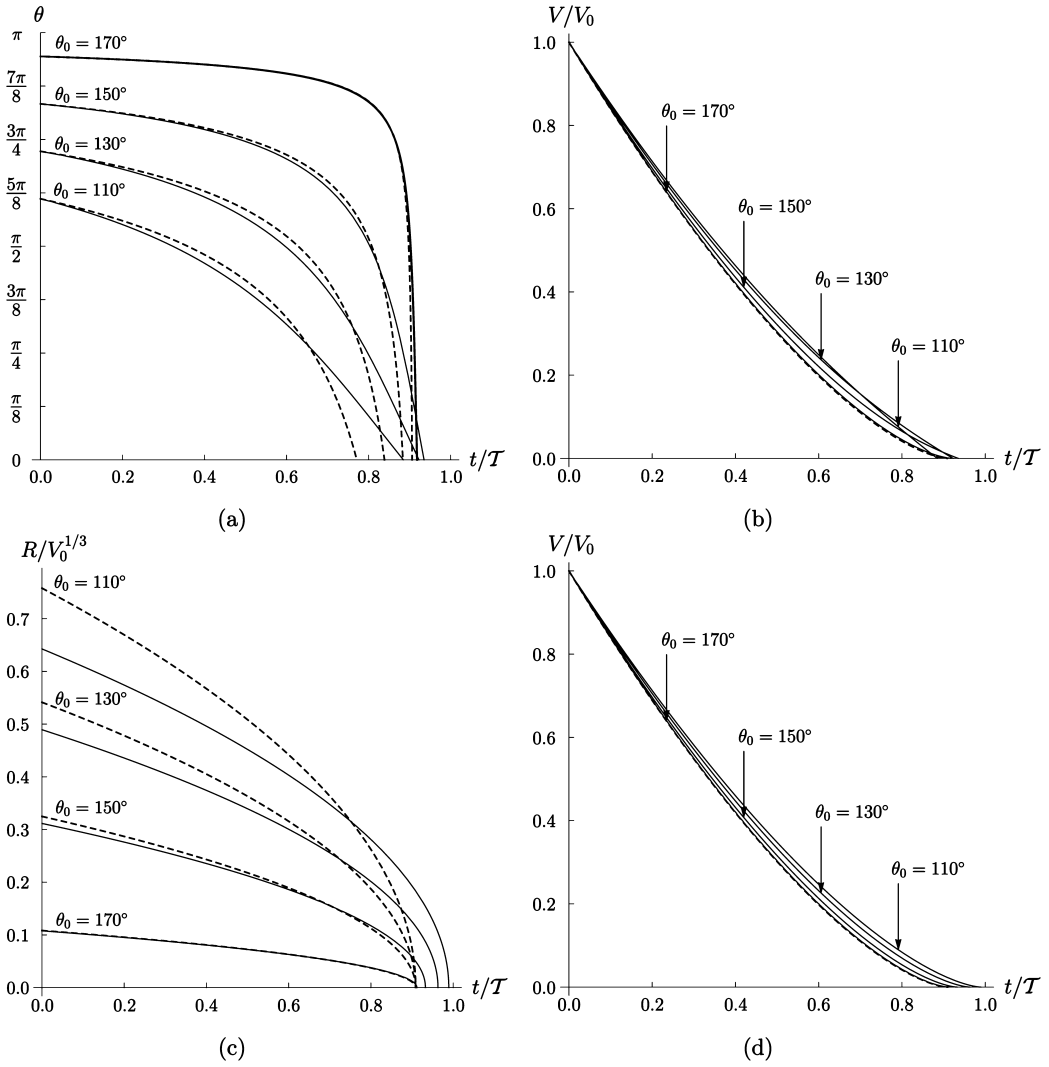

Figure 4. Evolutions of (a) the contact angle θ and (b) the scaled volume V/V_0 for a droplet evaporating in the CR mode, and evolutions of (c) the scaled contact radius $R/V_0^{1/3}$ and (d) the scaled volume V/V_0 for a droplet evaporating in the CA mode, plotted as functions of scaled time $t/\mathcal{T}$ for droplets on hydrophobic substrates with different initial contact angles, namely, $\theta_0 = 11\pi/18 = 110°$, $\theta_0 = 13\pi/18 = 130°$, $\theta_0 = 5\pi/6 = 150°$, and $\theta_0 = 17\pi/18 = 170°$, together with the corresponding asymptotic expressions in the limit $\theta_0 \to \pi^-$ given by eqs 26−28 shown with dashed lines.

value of θ_0 they are virtually indistinguishable. Specifically, eqs 26 and 27 reveal that, whichever mode the droplet is evaporating in, the asymptotic expression for the droplet volume V is given by

$$V = V_0\left(1 - \frac{t}{t_\pi}\right)^{3/2} + O(\pi - \theta_0)^2 \tag{28}$$

in the limit $\theta_0 \to \pi^-$.

The increasing accuracy of the asymptotic expressions 26−28 as θ_0 increases toward π is illustrated in Figure 4, which shows the evolutions of θ and V/V_0 for a droplet evaporating in the CR mode, and the evolutions of $R/V_0^{1/3}$ and V/V_0 for a droplet evaporating in the CA mode, plotted as functions of $t/\mathcal{T}$ for droplets on hydrophobic substrates with different initial contact angles, namely, $\theta_0 = 11\pi/18 = 110°$, $\theta_0 = 13\pi/18 = 130°$, $\theta_0 = 5\pi/6 = 150°$, and $\theta_0 = 17\pi/18 = 170°$, together with the corresponding asymptotic expressions in the limit $\theta_0 \to \pi^-$ given by eqs 26−28. In particular, Figure 4a,c shows that the asymptotic expressions 27 and 26 provide good approximations to the evolutions of θ and R, respectively, when θ_0 is greater than about 150°, and Figure 4b,d shows that the asymptotic expression 28 provides a good approximation to the evolutions of V in *both* modes for all of the values of θ_0 shown.

One important consequence of the convergence of the extreme modes is that using the exact solution for the evolution of V in the CA mode given by eq 16, which predicts the so-called "2/3 power law" that $(V/V_0)^{2/3}$ varies linearly with t, to extrapolate experimental data for V to estimate the lifetime of a droplet (as was done by, for example, Nguyen et al.,[32] Nguyen and Nguyen,[33] and Stauber et al.[10]), is also valid for the CR mode provided that θ_0 is sufficiently close to π. This conclusion is entirely consistent with the recent work of Nguyen and Nguyen,[34] who found that evolution of V in the CR mode is well approximated by the 2/3 power law when θ_0 is sufficiently close to π.

5. SUMMARY AND CONCLUSIONS

In the present work we have described the manner in which the extreme modes of droplet evaporation become indistinguishable on strongly hydrophobic substrates. In particular, we obtained simple asymptotic expressions 26−28 which provide good approximations to the evolutions of R, θ, and V, respectively, for a

DOI: 10.1021/acs.langmuir.5b00286
Langmuir 2015, 31, 3653−3660

wide range of hydrophobic substrates. As a consequence, on strongly hydrophobic substrates it is appropriate to use the 2/3 power law to extrapolate the lifetimes of droplets evaporating in the CR mode as well as in the CA mode.

As pointed out in Section 2, the present analysis is based on the simplest and most widely used version of the diffusion-limited model in which the saturation value of the vapor concentration, c_{sat}, is assumed to be constant. The predictions of this version of the model have been found to be in excellent agreement with experimental results by many authors, including Picknett and Bexon,[4] Coutant and Penski,[11] Erbil et al.,[14] Shin et al.,[21] Doganci et al.,[26] Gelderblom et al.,[27] Sobac and Brutin,[29] Song et al.,[31] Nguyen et al.,[32] Nguyen and Nguyen,[6,33] Talbot et al.,[35] Dash and Garimella,[8,37] Semenov et al.,[24,25] Trybala et al.,[38] and Stauber et al.[10] However, in reality, the value of c_{sat} depends on temperature, and so in situations in which evaporative cooling of the free surface of the droplet becomes significant it may be necessary to extend the model to include variations in c_{sat}. For example, Dunn et al.[17] and Sefiane et al.[20] used this approach to analyze the effects of the conductivity of the substrate and of the pressure in the atmosphere above the droplet. In particular, since instantaneous evaporative cooling increases with the instantaneous contact angle of the droplet (see, for example, the work of Dash and Garimella[8]) it may become significant as the initial contact angle increases toward π (i.e., on hydrophobic and superhydrophobic substrates). In particular, two recent investigations of the evaporation of droplets of water on different superhydrophobic substrates have reached different conclusions about the significance of evaporative cooling. Whereas Gelderblom et al.[27] found good agreement between the predictions of the simplest version of the model and their experiments on a substrate with an initial contact angle of up to $\theta_0 \simeq 150°$, Dash and Garimella[8] observed significant evaporative cooling on a substrate with an initial contact angle of $\theta_0 \simeq 160°$ and proposed an ad hoc modification of the simplest version of the model (namely, reducing the theoretical prediction of the total evaporative flux by an empirically determined factor of 20%) to account for it. Recently Gleason and Putnam[39] proposed another ad hoc modification of the simplest version of the model (namely, incorporating a prescribed temperature distribution of the free surface of the droplet) to account for the evaporative cooling of a droplet on a heated substrate. However, since the instantaneous evaporative cooling depends on the instantaneous geometry of the droplet, its instantaneous effect will be the same on both extreme modes. Hence we hypothesize that, even in situations such as those studied by Dash and Garimella[8] in which evaporative cooling is significant, the main result of the present work, namely, that the extreme modes become indistinguishable on strongly hydrophobic substrates, will still hold true.

AUTHOR INFORMATION

Corresponding Author

*E-mail: s.k.wilson@strath.ac.uk.

Notes

The authors declare no competing financial interest.

ACKNOWLEDGMENTS

J.M.S. gratefully acknowledges the financial support of the United Kingdom Engineering and Physical Science Research Council (EPSRC), the University of Strathclyde, and the University of Edinburgh via a postgraduate research studentship. This work was undertaken while S.K.W. was a Leverhulme Trust Research Fellow (2013−16) supported by Award RF-2013-355 "Small Particles, Big Problems: Understanding the Complex Behaviour of Nanofluids".

REFERENCES

(1) Cazabat, A.-M.; Guéna, G. Evaporation of macroscopic sessile droplets. *Soft Matter* **2010**, *6*, 2591−2612.

(2) Erbil, H. Y. Evaporation of pure liquid sessile and spherical suspended drops: A review. *Adv. Colloid Interface Sci.* **2012**, *170*, 67−86.

(3) Larson, R. G. Transport and deposition patterns in drying sessile droplets. *AIChE J.* **2014**, *60*, 1538−1571.

(4) Picknett, R. G.; Bexon, R. The evaporation of sessile or pendant drops in still air. *J. Colloid Interface Sci.* **1977**, *61*, 336−350.

(5) Bourgès-Monnier, C.; Shanahan, M. E. R. Influence of evaporation on contact angle. *Langmuir* **1995**, *11*, 2820−2829.

(6) Nguyen, T. A. H.; Nguyen, A. V. Increased evaporation kinetics of sessile droplets by using nanoparticles. *Langmuir* **2012**, *28*, 16725−16728.

(7) Nguyen, T. A. H.; Nguyen, A. V. Reply to Comment on "Increased evaporation kinetics of sessile droplets by using nanoparticles". *Langmuir* **2013**, *29*, 12330.

(8) Dash, S.; Garimella, S. V. Droplet evaporation dynamics on a superhydrophobic surface with negligible hysteresis. *Langmuir* **2013**, *29*, 10785−10795.

(9) Stauber, J. M.; Wilson, S. K.; Duffy, B. R.; Sefiane, K. Comment on "Increased evaporation kinetics of sessile droplets by using nanoparticles". *Langmuir* **2013**, *29*, 12328−12329.

(10) Stauber, J. M.; Wilson, S. K.; Duffy, B. R.; Sefiane, K. On the lifetimes of evaporating droplets. *J. Fluid Mech.* **2014**, *744*, R2.

(11) Coutant, R. W.; Penski, E. C. Experimental evaluation of mass transfer from sessile drops. *Ind. Eng. Chem. Fundam.* **1982**, *21*, 250−254.

(12) Deegan, R. D.; Bakajin, O.; Dupont, T. F.; Huber, G.; Nagel, S. R.; Witten, T. A. Capillary flow as the cause of ring stains from dried liquid drops. *Nature* **1997**, *389*, 827−829.

(13) Deegan, R. D.; Bakajin, O.; Dupont, T. F.; Huber, G.; Nagel, S. R.; Witten, T. A. Contact line deposits in an evaporating drop. *Phys. Rev. E* **2000**, *62*, 756−765.

(14) Erbil, H. Y.; McHale, G.; Newton, M. I. Drop evaporation on solid surfaces: Constant contact angle mode. *Langmuir* **2002**, *18*, 2636−2641.

(15) Hu, H.; Larson, R. G. Evaporation of a sessile droplet on a substrate. *J. Phys. Chem. B* **2002**, *106*, 1334−1344.

(16) Popov, Y. O. Evaporative deposition patterns: Spatial dimensions of the deposit. *Phys. Rev. E* **2005**, *70*, 036313.

(17) Dunn, G. J.; Wilson, S. K.; Duffy, B. R.; David, S.; Sefiane, K. The strong influence of substrate conductivity on droplet evaporation. *J. Fluid Mech.* **2009**, *623*, 329−351.

(18) Dunn, G. J.; Wilson, S. K.; Duffy, B. R.; Sefiane, K. Evaporation of a thin droplet on a thin substrate with a high thermal resistance. *Phys. Fluids* **2009**, *21*, 052101.

(19) Masoud, H.; Felske, J. D. Analytical solution for inviscid flow inside an evaporating sessile drop. *Phys. Rev. E* **2009**, *79*, 016301.

(20) Sefiane, K.; Wilson, S. K.; David, S.; Dunn, G. J.; Duffy, B. R. On the effect of the atmosphere on the evaporation of sessile droplets of water. *Phys. Fluids* **2009**, *21*, 062101.

(21) Shin, D. H.; Lee, S. H.; Jung, J.-Y.; Yoo, J. Y. Evaporating characteristics of sessile droplet on hydrophobic and hydrophilic surfaces. *Microelectron. Eng.* **2009**, *86*, 1350−1353.

(22) Eggers, J.; Pismen, L. M. Nonlocal description of evaporating drops. *Phys. Fluids* **2010**, *22*, 112101.

(23) Semenov, S.; Starov, V. M.; Rubio, R. G.; Velarde, M. G. Instantaneous distribution of fluxes in the course of evaporation of sessile liquid droplets: Computer simulations. *Colloids Surf. A* **2010**, *372*, 127−134.

(24) Semenov, S.; Trybala, A.; Agogo, H.; Kovalchuk, N.; Ortega, F.; Rubio, R. G.; Starov, V. M.; Velarde, M. G. Evaporation of droplets of surfactant solutions. *Langmuir* **2013**, *29*, 10028−10036.

DOI: 10.1021/acs.langmuir.5b00286
Langmuir 2015, 31, 3653−3660

(25) Semenov, S.; Trybala, A.; Rubio, R. G.; Kovalchuk, N.; Starov, V. [M.]; Velarde, M. G. Simultaneous spreading and evaporation: Recent developments. *Adv. Colloid Interface Sci.* **2014**, *206*, 382−398.
(26) Doganci, M. D.; Sesli, B. U.; Erbil, H. Y. Diffusion-controlled evaporation of sodium dodecyl sulfate solution drops placed on a hydrophobic substrate. *J. Colloid Interface Sci.* **2011**, *362*, 524−531.
(27) Gelderblom, H.; Marín, ÁG.; Nair, H.; van Houselt, A.; Lefferts, L.; Snoeijer, J. H.; Lohse, D. How water droplets evaporate on a superhydrophobic substrate. *Phys. Rev. E* **2011**, *83*, 026306.
(28) Gelderblom, H.; Bloemen, O.; Snoeijer, J. H. Stokes flow near the contact line of an evaporating drop. *J. Fluid Mech.* **2012**, *709*, 69−84.
(29) Sobac, B.; Brutin, D. Triple-line behavior and wettability controlled by nanocoated substrates: Influence on sessile drop evaporation. *Langmuir* **2011**, *27*, 14999−15007.
(30) Sobac, B.; Brutin, D. Thermal effects of the substrate on water droplet evaporation. *Phys. Rev. E* **2012**, *86*, 021602.
(31) Song, H.; Lee, Y.; Jin, S.; Kim, H. Y.; Yoo, J. Y. Prediction of sessile drop evaporation considering surface wettability. *Microelectron. Eng.* **2011**, *88*, 3249−3255.
(32) Nguyen, T. A. H.; Nguyen, A. V.; Hampton, M. A.; Xu, Z. P.; Huang, L.; Rudolph, V. Theoretical and experimental analysis of droplet evaporation on solid surfaces. *Chem. Eng. Sci.* **2012**, *69*, 522−529.
(33) Nguyen, T. A. H.; Nguyen, A. V. On the lifetime of evaporating sessile droplets. *Langmuir* **2012**, *28*, 1924−1930.
(34) Nguyen, T. A. H.; Nguyen, A. V. Transient volume of evaporating sessile droplets: 2/3, 1/1, or another power law? *Langmuir* **2014**, *30*, 6544−6547.
(35) Talbot, E. L.; Berson, A.; Brown, P. S.; Bain, C. D. Evaporation of picoliter droplets on surfaces with a range of wettabilities and thermal conductivities. *Phys. Rev. E* **2012**, *85*, 061604.
(36) Yu, Y.-S.; Wang, Z.; Zhao, Y.-P. Experimental and theoretical investigations of evaporation of sessile water droplet on hydrophobic surfaces. *J. Colloid Interface Sci.* **2012**, *365*, 254−259.
(37) Dash, S.; Garimella, S. V. Droplet evaporation on heated hydrophobic and superhydrophobic surfaces. *Phys. Rev. E* **2014**, *89*, 042402.
(38) Trybala, A.; Okoye, A.; Semenov, S.; Agogo, H.; Rubio, R. G.; Ortega, F.; Starov, V. M. Evaporation kinetics of sessile droplets of aqueous suspensions of inorganic nanoparticles. *J. Colloid Interface Sci.* **2013**, *403*, 49−57.
(39) Gleason, K.; Putnam, S. A. Microdroplet evaporation with a forced pinned contact line. *Langmuir* **2014**, *30*, 10548−10555.
(40) Gatapova, E. Y.; Semenov, A. A.; Zaitsev, D. V.; Kabov, O. A. Evaporation of a sessile water drop on a heated surface with controlled wettability. *Colloids Surf. A* **2014**, *441*, 776−785.
(41) Lebedev, N. N. *Special Functions and their Applications*; Prentice Hall, Inc.: Upper Saddle River, NJ, 1965.
(42) Smith, G. S.; Barakat, R. Electrostatics of two conducting spheres in contact. *Appl. Sci. Res.* **1975**, *30*, 418−432.

DOI: 10.1021/acs.langmuir.5b00286
Langmuir 2015, 31, 3653−3660